An InGaP/GaAs Resonant-Tunnelling Bipolar Transistor (RTBT) with Multiple Negative-Differential-Resistance (MNDR) Phenomena

H. M. Chuang
Inst. of Microelectronics, Dept .of Electrical Engineering, National Cheng-Kung University, Taiwan

K. W. Lin
Inst. of Microelectronics, Dept .of Electrical Engineering, National Cheng-Kung University, Taiwan

H. J. Pan
Inst. of Microelectronics, Dept .of Electrical Engineering, National Cheng-Kung University, Taiwan

K. M. Lee
Inst. of Microelectronics, Dept .of Electrical Engineering, National Cheng-Kung University, Taiwan

X. D. Liao
Inst. of Microelectronics, Dept .of Electrical Engineering, National Cheng-Kung University, Taiwan

W. C. Liu*
Inst. of Microelectronics, Dept .of Electrical Engineering, National Cheng-Kung University, Taiwan
wcliu@mail.ncku.edu.tw

Abstract

An InGaP/GaAs resonant tunnelling bipolar transistor (RTBT) with superlattice (SL) in the emitters is fabricated and studied. The modulated widths of SL barriers are utilized in the specific SL structure. Based on the calculations, the ground state and first excited state minibands are estimated from the transmission probability. The electron transport of RT through SL structure is significantly determined by the electric field behaviors across SL barriers. Experimentally, the excellent transistor characteristics including the small saturation voltage, small offset voltage, high breakdown voltages are obtained due to the insertion of ¢-doping sheet at the base-collector heterointerface. Furthermore, at higher current regimes, the quaternary negative difference resistance (NDR) phenomena are observed in agreement with the theoretical prediction at 300K.

1. Introduction

In recent years, significant advances in semiconductor devices have caused the rapid development of circuit performances. Following the appearance of quantum devices with carrier transport of resonant tunnelling (RT), dramatic improvements in circuit performances are further achieved as a result of the picoseconds switching speed and multi-function [1-2]. Among these RT devices, resonant tunnelling bipolar transistors (RTBTs), taking advantages of the high current handling capability and high current gain, are promising in digital applications [3]. From the viewpoint of high-speed and low-power requirements, the vertical integration of RT and three-terminal transistor structures reduces the signal delay and power dissipation effectively. Previously, several attempts were made on the RT structures to obtain multiple negative differential resistance (MNDR) characteristics. Liu et al. demonstrated the AlGaAs/GaAs superlattice (SL)-emitter RTBT with a high current gain of about 60 under low temperature operation [4--5]. The "quasi-DBQW" operation utilizes two minibands in the SL-emitter serving as the sequential tunneling paths and results in the double NDR characteristics.

In this work, we demonstrate the room temperature operation of an InGaP/GaAs SL-emitter RTBT with observations of NDR phenomena. As compared to the AlGaAs/GaAs material system, the InGaP/GaAs system is more suitable for superlattice applications since the normal InGaP/GaAs and inverted GaAs/InGaP interfaces are both smooth on the atomic scale. Based on the concept of transmission delay through SL structures, the electron transport paths are determined by the electric field behaviors. These can be characterized by two electron transport mechanisms through sequential miniband conduction of RT. On the other hand, in order to eliminate the undesired electron transport properties across base-collector (B-C) heterojunction resulting from the employment of wide-gap collector, a δ-doping sheet sandwiched between two spacers is utilized. Experimentally, the studied device exhibits excellent transistor characteristics including the high current gain, high breakdown voltage, low saturation voltage, and low offset voltage. Furthermore, at higher current regimes, the quaternary-NDR characteristic resulting from the distinct RT conduction is observed.

2. Device Fabrication

The studied device was grown by a low-pressure metal organic chemical vapor deposition (LP-MOCVD) system on an n^+-GaAs substrate. Silicon and zinc were used as the n-type and p-type dopants, respectively. The schematic cross section of the device is illustrated in Fig. 1. The detailed epitaxial layers consisted of a 2000Å $n^+=3x10^{18}cm^{-3}$ GaAs buffer, a 5000Å $n^-=2x10^{16}cm^{-3}$ $In_{0.5}Ga_{0.5}P$ collector, a 30Å undoped GaAs spacer, a $\delta(n^+)=2x10^{12}cm^{-2}$ doping sheet, a 30Å undoped GaAs spacer, a 700Å $p^+=1x10^{19}cm^{-3}$ GaAs base, a 300Å $n=5x10^{17}cm^{-3}$ GaAs emitter, a 5-period i-$In_{0.5}Ga_{0.5}P$/n-GaAs SL structure and a 2000Å GaAs cap layer ($n^+=1x10^{18}cm^{-3}$). In the SL structures, the device had the undoped $In_{0.5}Ga_{0.5}P$ barriers with barrier width of 50Å except the first and last barriers were designed to be 25Å. The width and concentration of n-GaAs well were 80Å and $1x10^{18}cm^{-3}$, respectively. After epitaxial growth, the studied device was fabricated by using conventional photolithography, vacuum evaporation, chemical wet etching, and lift-off techniques. By means of the chemical etching selectivity between InGaP and GaAs layers, the ledge technology was utilized by a 300Å-thick completely depleted GaAs emitter as the passivation layer. The emitter and collector contacts were formed by using AuGe alloys as the metallization, and AuZn for the base contact. The available emitter area of $20x20\mu m^2$ was utilized in both the studied devices.

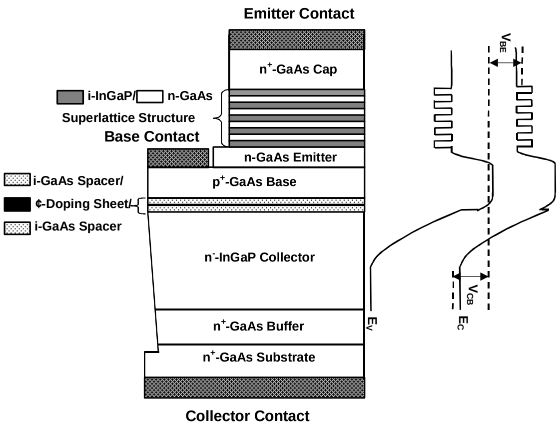

Figure 1. Schematic cross section of the basic structure and energy band diagram under normal transistor operation

3. Results and Discussion

The typical common-emitter I-V characteristics of the studied device measured at low collector current regimes are illustrated in Fig. 2. Obviously, the abrupt rise of current in I-V characteristics gives a good evidence of the near ideal current transport across B-C heterojunction in presence of δ-doping sheet. From Fig. 2, a small saturation voltage of 0.5V is found at the collector current level of 3.2mA. When using RTBT in digital logic applications, this superior saturation property is a great benefit to acquire the stability of threshold characteristics. On the other hand, a low collector-emitter offset voltage smaller than 150mV supports the symmetric electron transport property for both junctions. The small offset voltage along with the small saturation voltage can remarkably reduce the power consumption in saturation logic circuits. Furthermore, owing to the merit of InGaP collector, the common-base and common-emitter breakdown voltages BV_{CBO} and BV_{CEO} can reach as high as 31V and 23V, respectively. These high breakdown performances show the potential in power applications.

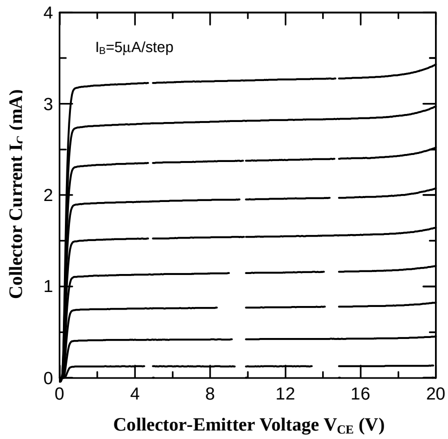

Figure 2. Common-emitter current-voltage characteristic at low current regimes at 300K

The normal transistor operation of the devices studied can be easily understood with the help of the energy band diagram shown in Fig. 1. Most of the applied base-emitter voltage V_{BE} is dropped across the emitter-base (E-B) depletion region until the flat-band condition between the emitter and base is achieved. As considering the electron transport through the strongly coupled SL structure, meanwhile, the electron envelope function in each well interacts substantially with adjacent well ones. According to the exact solution of Schrödinger's equation, the envelope function can be expressed by the linear combination of incident and reflected plane waves.

Figure 3 shows the energy dependence of transmission probability T(E) through the SL structures designed of both devices without applied bias. The first and second resonance, for both devices, occurs at the ground-state miniband of E_1=40meV and the excited-state miniband of E_2=150meV calculated from the bottom of the well, respectively. Figure 4 presents the measured transfer characteristic at 300K for a fixed collector-emitter voltage V_{CE} of 3V. Clearly, four current peaks are considered to be dominated by a specific electron transport mechanism in presence of uniform field distribution. Figure 5 depicts the sequence of potential profile of SL under various bias conditions. As a sufficiently small bias is applied across the SL, the consistent low-field domains are formed over each barrier. It is noted that the field across wells can be ignored due to the n-type doping level in quantum wells. As depicted in Fig. 5(a), the resonance occurs through ground-state miniband conduction until the potential over each barrier is higher than $\gamma \hbar / \tau_1$ where γ is a constant of order unity. The tunneling component which reaches to the maximum value is comparable with the thermionic emission one. At the same time, as a result of the accumulation of a fraction of transferring electrons from well to well, the space-charge buildup induced screening effect of the field is manifest. When the bias is increased, the additional portion develops high-field domains and the formation of high-field domain appears at first over the barrier adjacent to the emitter side and then extends one after the other toward the cap layer. From Fig. 5(b), (c) and (d), the resonance occurs through the sequential conduction between E_1 and E_2 in the wells and causes the expected multiple NDR phenomena. The voltage differences between two adjacent current peaks of 0.12, 0.11 and 0.14V, as found in Fig. 4, give a good evidence to be consistent with the value of E_2-E_1. Figure 6 illustrates the common-emitter I-V characteristics (300K) at higher current levels. Four regimes of collector current drops are found as I_B is increased from 0.24 to 0.28, 0.32 to 0.36, 0.4 to 0.52, and 0.56 to 0.6mA, respectively. Since the RT conduction is mainly dominated by the V_{BE} bias, the collector current regimes where the NDR phenomena observed are approximate to the observation in the transfer I-V characteristics of Fig. 4.

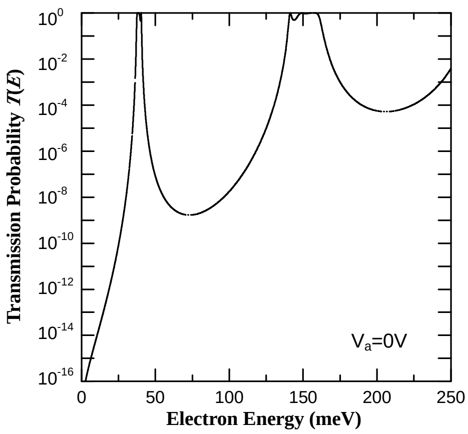

Figure 3. Calculated transmission probability as a function of electron energy through the unbiased superlattice

4. Conclusions

We have demonstrated and investigated the electron transport properties of an InGaP/GaAs RTBT utilizing superlattice as the RT structures in the emitters. With the design of barrier width, the transmission delay occurring in the external barriers dominates the electric field

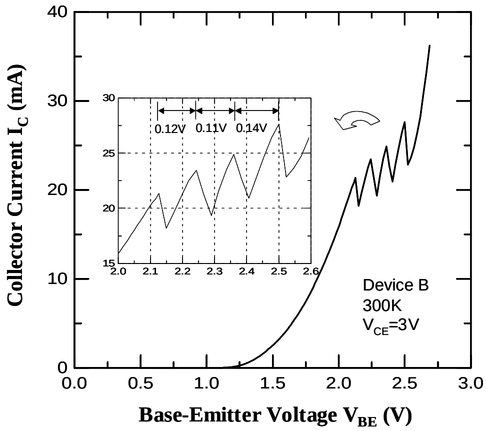

Figure 4. Transfer current-voltage characteristics measured at 300K and a fixed collector-emitter voltage of V_{CE}=3V

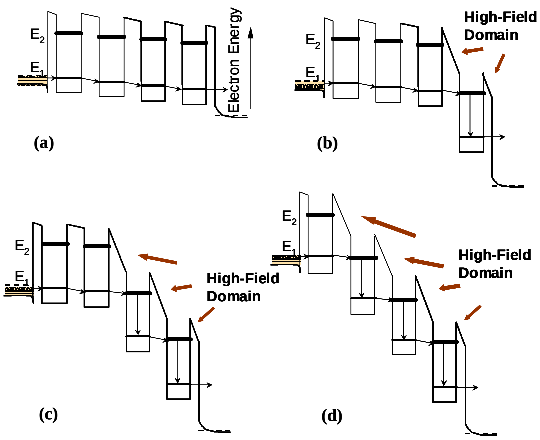

Figure 5. Schematic potential profiles of the superlattice regime for device B under different biases

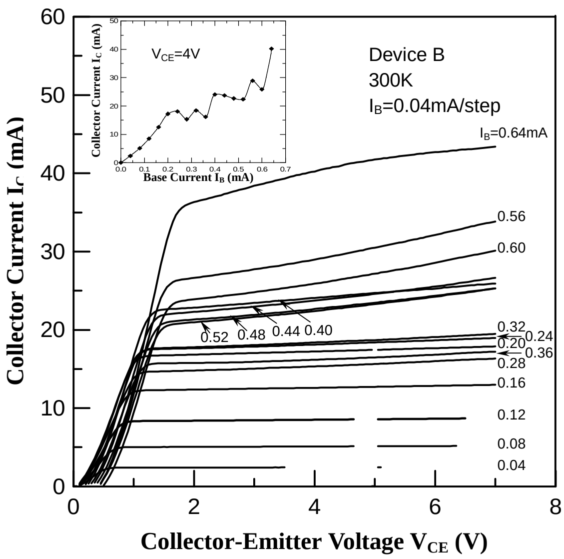

Figure 6. Common-emitter current-voltage characteristics at 300K. The respective insets show the plots of I_C versus I_B at a fixed collector-emitter voltage of V_{CE}=4V.

behaviors across the SL structures. The observation of quaternary-NDR phenomena in I-V characteristics at 300K is associated with two paths of RT conduction through two minibands. Furthermore, with a wide-gap collector, the breakdown voltage larger than 20V is obtained for transistor operations. The introduction of a δ-doping sheet also provides good saturation properties by eliminating the non-ideal effect of electron transport across the B-C heterojunction.

References

[1] W. Williamson, III, S. Enquist, D. Chow, H. Dunlap, S. Subramaniam, P. Lei, G. B. Gilbert, “12GHz clocked operation of ultra low power interband resonant tunneling diode pipelined logic gates,” IEEE J. Solid-State Circuits, vol. 32, pp. 222- 231, 1997.

[2] P. Mazumder, S. Kulkarni, M. Bhattacharya, J. P. Sun, and G. I. Haddad, “Digital circuit applications of resonant tunneling devices,” IEEE Proc., vol. 86, pp. 664 –686, 1998.

[3] G. Haddad, “Resonant tunneling heterojunction bipolar transistors and their applications in high functionality/speed digital circuits,” in Proc. 8th Int. Conf. Indium Phosphide and Related Materials, 1996, pp. 129-132.

[4] W. C. Liu, W. S. Lour, and Y. H. Wang, “Investigation of AlGaAs/GaAs superlattice-emitter resonant tunneling bipolar transistor (SE-RTBT),” IEEE J. Solid-State Circuits, vol. 27, pp. 2214- 2219, 1992.

[5] W. C. Liu and W. S. Lour, “Negative-differential-resistance (NDR) superlattice-emitter transistor,” Jpn. J. Appl. Phys., vol. 30, pp. L564-567, 1991.